

Switching particle systems for foraging ants showing phase transitions in path selections

Ayana Ezoe¹, Saori Morimoto¹, Yuya Tanaka¹, Makoto Katori¹ *
and Hiraku Nishimori² †

8 April 2024

Abstract

Switching interacting particle systems studied in probability theory are the stochastic processes of hopping particles on a lattice made up of slow and fast particles, where the switching between these types of particles occurs randomly at a given transition rate. This paper explores how such stochastic processes involving multiple particles can model group behaviors of ants. Recent experimental research by the last author's group has investigated how ants switch between two types of primarily relied cues to select foraging paths based on the current situation. Here, we propose a discrete-time interacting random walk model on a square lattice, incorporating two types of hopping rules. Numerical simulation results demonstrate global changes in selected homing paths, transitioning from trailing paths of the 'pheromone road' to nearly optimal paths depending on the switching parameters. By introducing two types of order parameters characterizing the dependence of homing duration distributions on switching parameters, we discuss these global changes as phase transitions in ant path selections. We also study critical phenomena associated with continuous phase transitions.

Keywords: Switching interacting particle systems; Group behaviors of ants; Switching of cues in foraging path selections; Interacting random walk model; Order parameters; Phase transitions and critical phenomena

*¹ Department of Physics, Faculty of Science and Engineering, Chuo University, Kasuga, Bunkyo-ku, Tokyo 112-8551, Japan; makoto.katori.mathphys@gmail.com

†² Meiji Institute for Advanced Study of Mathematical Sciences, Meiji University, Nakano, Nakano-ku, Tokyo 164-8525, Japan; e-mail: nishimor2@meiji.ac.jp

1 Introduction

For reaction-diffusion systems with *double diffusivity*, the interacting particle systems in one dimension were introduced as microscopic models, in which we have two types of particles; *fast particles* and *slow particles* [4]. Fast particles hop at rate 1 and slow particles at rate $\epsilon \in [0, 1)$. Switching between two types of particles occurs at rate $\gamma \in (0, \infty)$. An alternative view of the models is to consider two layers of particles such that the hopping rate for the bottom layer is 1, whereas that for the top layer is $\epsilon < 1$, and to let particles change layers at rate γ . It is noteworthy that the motivation for studying such switching particle systems came from population genetics [4]. Individuals living in colonies can behave either *active* or *dormant*. The active individuals undergo clonal reproduction by resampling within a colony and migrate between colonies via hopping. They can become dormant and then resampling and migration are suspended until they become active again. Dormant individuals reside in *seed banks*. A useful review of the important roles of dormancy in life sciences was provided by [8]. In switching interacting particle systems, the active (resp. dormant) individuals are represented by fast (resp. slow) particles. Other mathematical models and their analyses for population dynamics with seed banks, see [2, 3, 5, 6].

This study aims to show the usefulness of the notion of switching interacting particle systems for modeling group behaviors for ant foraging [7, 10]. The group behaviors of so-called *eusocial insects* (*e.g.* ants, bees, and termites) have been of interest not only in biology [7] but also in statistical physics as many-body phenomena in systems consisting of interacting, permanently moving units. Although persistent motion is a common feature of living systems, recently several physical and chemical systems comprising interacting *self-propelled* units have been reported. *Interacting self-propelled particle systems* exhibit richer phenomena in their collective motion than the thermal or chemical fluctuation phenomena in equilibrium systems. Study of collective motions of self-propelled particles in both living and non-living worlds is now one of the most active and fruitful topics in non-equilibrium statistical physics [12]. Through direct and indirect communication, ants in colonies share various types of information and exhibit highly organized group behaviors which enable them to perform complex tasks [7]. Foraging is one of the most intensively studied subjects in such interesting group behaviors [10, 12].

1.1 Switching particle systems modeling individual switching behaviors

Recruit pheromone is a chemical substance or mixture released by an organism that influences the behaviors of other individuals. Various species of ants establish lengthy foraging trails through a positive feedback process involving the secretion and tracking of recruit pheromone, enabling them to efficiently shuttle between the nest and food sources. However, a recent combined study of experiments and mathematical modeling for a species of garden ant suggested a situation-dependent switch of the primarily relied cues from chemical ones (*e.g.* recruit pheromone) to other ones, most likely visual cues. Here, visual cues refer to landmarks, the polarization angle of the sun or moon, textures of the edges of crowded

plants or woods, and other visual stimuli [10].

To elucidate the sudden changes of path patterns of ant trails which were experimentally observed depending on geometric configuration of the nest and food source on a plane (see Section 1.2 below), Ogiwara *et al.* proposed a multi-agent model [10]. In this model, foraging ants are depicted as biased random walkers on a lattice with their probabilities of hopping to nearest neighboring sites weighted based on the evolving pheromone field over time. The local intensity of the pheromone field increases through pheromone secretion by exploring ants and homing ants (with the pheromone field diminishing due to constant evaporation). In addition to such a *pheromone-mediated walk* of ants, a *visual-cues-mediated walk* is considered for homing ants, which aims to achieve an optimal path to the nest. They introduced a parameter α for each ant at each time, which measures the conflict between the optimal path and the redundant path made by pheromone-mediated walk [10]. To make switching from the pheromone-mediated walk to the visual-cues-mediated walk, they assumed a critical value α_c , and when $\alpha > \alpha_c$ the switching occurs and the direction of the hopping is aligned toward the nest.

In this paper, we propose another mathematical model for the selection of foraging paths by ants inspired by the concept of switching interacting particle systems [4]. We consider a discrete-time interacting random walk model of hopping particles on a square lattice (a cellular automaton model) [1, 9]. The ants exploring outward from the nest to the food source are depicted as random walkers during the *exploring period*, while those returning from the food source to nest are portrayed as random walkers during the *homing period*. We regard the exploring and homing ants following the pheromone-mediated walk as slow particles, and the homing ants utilizing the visual-cues-mediated walk as fast particles:

$$\begin{aligned} \text{pheromone-mediated walk} &\iff \text{slow particle,} \\ \text{visual-cues-mediated walk} &\iff \text{fast particle.} \end{aligned} \tag{1.1}$$

During the exploring period, all particles are slow, whereas in the homing period, transitions can occur from slow particles to fast particles. These fast particles, representing “pioneering ants”, establish shorter paths to the nest. However, pioneering ants may face a *higher risk encountering enemies* compared to the ants following previously established paths. Therefore, fast particles should revert to slow particles to mitigate this risk. The switching between the two types of particle behavior occurs randomly at each time step as

$$\begin{aligned} \text{slow particle} &\implies \text{fast particle} && \text{with probability } \gamma_{\text{sf}}, \\ \text{fast particle} &\implies \text{slow particle} && \text{with probability } \gamma_{\text{fs}}. \end{aligned} \tag{1.2}$$

We will investigate how the global changes in homing paths depend on the parameters γ_{sf} and γ_{fs} . Notice that, since here we consider a discrete-time stochastic model, γ_{sf} and γ_{fs} are not transition rates but transition probabilities taking values in $[0, 1]$.

1.2 Experiments suggesting phase transitions

Now, we provide a concise overview of the experiments on forage path selection by ants conducted by the research group led by the last author of this paper (the Nishimori group).

These experiments provided clear evidence of the switching phenomenon in the primarily relied cues used by ants from recruit pheromone to visual information [10].

They utilized *Lasius Japonicus*, a species of garden ant found in Japan, raised in plastic boxes measuring $23 \times 12 \times 3.5$ cm equipped with special floors and walls covered in plaster to maintain internal humidity. Each box accommodated approximately 200 to 300 ants and was shielded by a black plate to shield the ants from light. Recruit pheromone was extracted from the remaining ants collected from the same natural colony using column chromatography. Experimental processes were recorded by a video camera. For further details on the setup, refer to the original paper [10].

In the box, a food source was placed at a separate position from the nest. They created a conflicting scenario where the homing directions for ants from the food source, as indicated by chemical cues and visual cues, diverged from each other as follows:

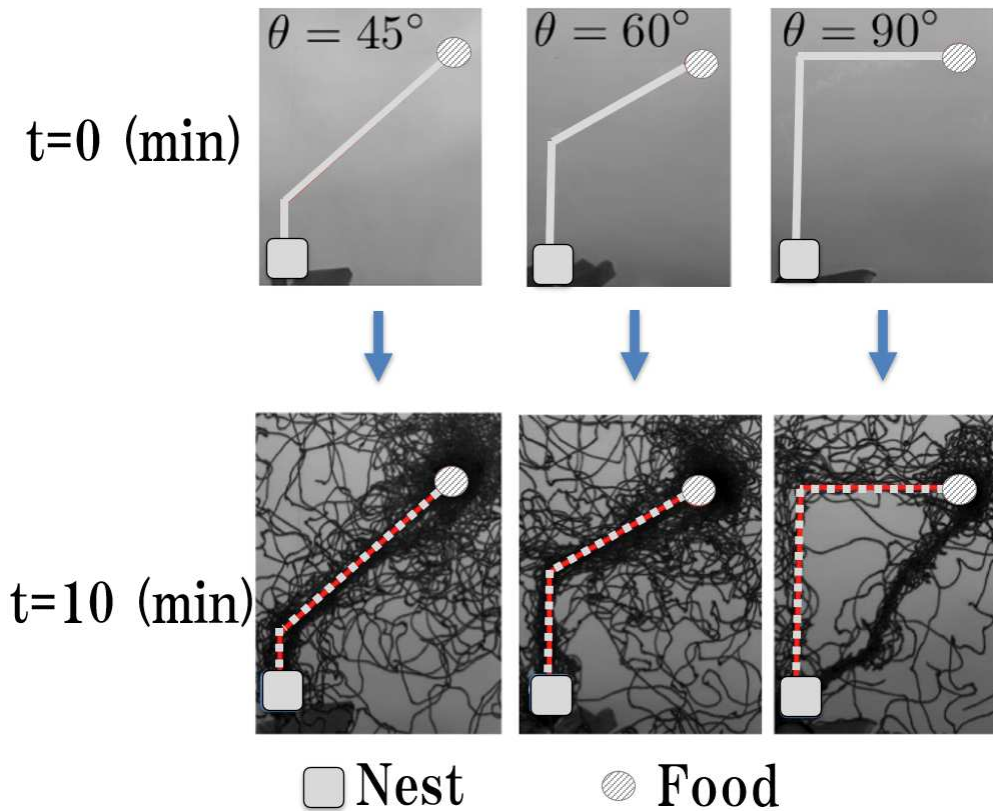


Figure 1: Three types of experimental settings and results for the observed paths of ants were reported by the Nishimori group.

1. At the beginning of each experiment, the preliminarily extracted recruit pheromone was applied along one of the three kinds of polygonal lines connecting the nest and the food source, which we call the ‘pheromone road’. One folding point was included in the lines with turning angles $\theta \in \{45^\circ, 60^\circ, 90^\circ\}$ (see Fig.1). The preliminarily extracted

pheromone had a sufficiently high density to maintain a strong attraction of ants until the end of each experiment.

2. From another experiment by the Nishimori group, it is considered that *Lasius Japonicus* can determine landmarks in the order of 10 cm [11]. Hence, ants in the present setup could recognize the direction of the nest from the food source. This direction along the optimal path from the food source to nest is different from the direction from the food sources indicated by the ‘pheromone road’ as mentioned above.

After getting food at the food source, ants start homing walk, and a conflict between the direction along the ‘pheromone road’ and the straight direction to the nest requires ants to make decision on which they rely chemical cues or visual cues. The degree α of this conflict becomes larger as angle θ increases.

The results are shown in Fig. 1. In the upper pictures, the initially prepared ‘pheromone roads’ are indicated by light-gray lines, each of them have a folding point with turning angle $\theta = 45^\circ, 60^\circ$, and 90° , respectively. Lower pictures show the trajectories of foraging ants recorded during the middle period (approximately 10 min) of each experiment with a duration of 60 min. Only in the case of $\theta = 90^\circ$, a direct path between the nest and food source was established, whereas in the other cases, no direct path was established until the end of the experiment at time $t = 60$ min.

It was claimed [10] that the change of the dominant path from the trailing paths of the ‘pheromone road’ to the direct path did not correspond to a continuous geometric change of the path. Instead, the direct path spontaneously emerged only in the case where $\theta = 90^\circ$.

The observation from the experiments above suggests that, if we introduce suitable parameters which control the individual motion of ants, there exist critical values of these parameters. The change in the dominant path can occur only within the ‘supercritical regime’ of these parameters. In this paper, we introduce two types of *order parameters* that characterize the global changes in the path patterns of foraging ants during homing walks from the food source to nest. Roughly speaking, they are given by

$$\begin{aligned} M &= \frac{\#\{\text{pioneering ants and their followers}\}}{\#\{\text{homing ants}\}}, \\ \widetilde{M} &= \frac{\#\{\text{ants trailing the ‘pheromone road’}\}}{\#\{\text{homing ants}\}}, \end{aligned} \tag{1.3}$$

where $\#\{\text{elements}\}$ denotes the total number of elements in a set $\{\text{elements}\}$. The precise definitions of M and \widetilde{M} are provided in Section 3. We also discuss the possibility of considering global changes in path patterns as *continuous phase transitions* associated with *critical phenomena* [1, 9, 12].

2 Discrete-time Stochastic Model on a Square Lattice

2.1 Switching random walks interacting through pheromone field

[General setting] Consider an $(L - 1) \times (L - 1)$ square region on a square lattice. The

set of vertices (sites) is given by

$$V_L := \{v = (x, y) : x \in \{0, 1, \dots, L-1\}, y \in \{0, 1, \dots, L-1\}\}. \quad (2.1)$$

We denote the Euclidean distance between two vertices $v_1, v_2 \in V_L$ as $|v_1 - v_2|$.

With discrete time

$$t \in \mathbb{N}_0 := \{0, 1, \dots\}, \quad (2.2)$$

we consider a set of random walks of a given number of particles, $N \in \mathbb{N} := \{1, 2, \dots\}$, on V_L . They are interacting with each other through the time-dependent pheromone field as explained below. However, we do not impose any exclusive interactions between particles. Hence, each vertex $v \in V_L$ can be occupied by any number of particles at each time.

The *nest* and *food sources* are assumed to be located at the origin $v_n := (0, 0)$ and the most upper-right vertex $v_f := (L-1, L-1)$, respectively.

All particles start at v_n successively from initial time $t = 0$ to $t = N-1$ and perform a drifted random walk toward v_f . After arriving at v_f , each particle immediately starts the drifted random walk from v_f toward v_n and then returns to v_n . In this way, the particles shuttle between v_n and v_f within a given period T . When a particle is in the time period for walking from v_n to v_f , we say that it is in an *exploring period*, and when it is in the time period for walking from v_f to v_n , it is said to be in a *homing period*.

We denote two types of hopping rules that represent the *slow mode* and *fast mode* of the drifted random walk, respectively. The particles are labeled by $j = 1, \dots, N$. At each time $t \in \mathbb{N}_0$, the state of the particle is specified by

the location : $v \in V_L$,
and the types of hopping : slow mode (s) or fast mode (f).

Hence, at each time $t \in \mathbb{N}_0$, the N -particle configuration is given by a set

$$X(t) := \{X_j(t) : j = 1, \dots, N\} \quad (2.3)$$

of the pairs of random variables,

$$X_j(t) = (v_j(t), \sigma_j(t)), \quad v_j(t) \in V_L, \quad \sigma_j(t) \in \{s, f\}, \quad (2.4)$$

$j = 1, \dots, N$. We define a discrete-time stochastic process, $(X(t))_{t \in \mathbb{N}_0}$.

[Time-dependent pheromone field]

The pheromone is placed on the vertices, and its intensity is expressed by a non-negative integer,

$$f(v, t) \in \mathbb{N}_0, \quad v \in V_L, \quad t \in \mathbb{N}_0. \quad (2.5)$$

That is, $f(v, t) = f \in \mathbb{N}_0$ implies that there are f units of pheromones on vertex $v \in V_L$ at time $t \in \mathbb{N}_0$. Define the Γ -shaped subset of V_L ,

$$\begin{aligned} \Gamma_{L,\ell} = & \{(x, y) \in V_L : 0 \leq x \leq \ell - 1, 0 \leq y \leq L - 1\} \\ & \cup \{(x, y) \in V_L : 0 \leq x \leq L - 1, L - \ell \leq y \leq L - 1\}. \end{aligned} \quad (2.6)$$

We will call $\Gamma_{L,\ell}$ the Γ -region, which represents the ‘pheromone road’. The variable ℓ indicates the *width of the Γ -region*. See Fig.2.

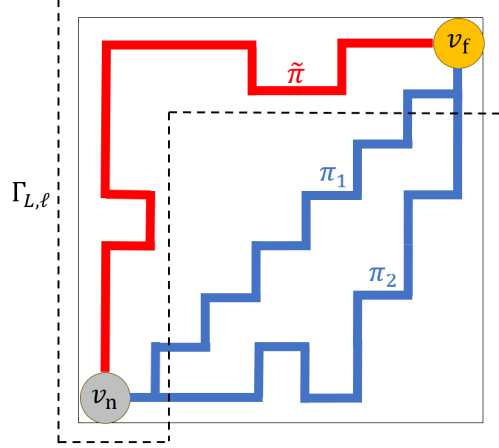


Figure 2: The setting of the model in the square region V_L is illustrated. Paths from the food source v_f to nest v_n during the homing period are classified. The path $\tilde{\pi}$ shown by the red line is an example of Γ -path which is completely included in the Γ -region, $\Gamma_{L,\ell}$. Two examples of nearly optimal paths are given by π_1 and π_2 , which are indicated by the blue lines. Some parts of the paths are outside $\Gamma_{L,\ell}$ and each homing duration A satisfies $2(L - 1) \leq A \leq 2(L - 1) + \langle \Delta A_0 \rangle / 2$.

With parameter $f_0 \in \mathbb{N}$, the initial value of the pheromone field is given by

$$f(v, 0) = \begin{cases} f_0, & \text{if } v \in \Gamma_{L,\ell}, \\ 0, & \text{if } v \in V_L \setminus \Gamma_{L,\ell}, \end{cases} \quad (2.7)$$

where $V_L \setminus \Gamma_{L,\ell}$ denotes the complement to $\Gamma_{L,\ell}$ in V_L . With the parameters $f_1, f_2 \in \mathbb{N}_0$, for each arrival of a particle at each vertex $v \in V_L$, the secretion of pheromones by an ant is represented by the following intensity increment,

$$f \rightarrow \begin{cases} f + f_1, & \text{in an exploring period,} \\ f + f_2, & \text{in a homing period.} \end{cases} \quad (2.8)$$

If $v \in V_L \setminus \Gamma_{L,\ell}$, each unit of the pheromone evaporates with probability q independently at each time step $t \rightarrow t + 1$. In other words, at time step $t \rightarrow t + 1$,

$$f \rightarrow f - n \quad \text{with probability} \quad \binom{f}{n} q^n (1 - q)^{f-n}, \quad n = 0, 1, \dots, f. \quad (2.9)$$

However, if $v \in \Gamma_{L,\ell}$, only the excess f over f_0 is evaporated. That is, if and only if $f > f_0$,

$$f \rightarrow f - n \quad \text{with probability} \quad \binom{f - f_0}{n} q^n (1 - q)^{f - f_0 - n}, \quad n = 0, 1, \dots, f - f_0. \quad (2.10)$$

[Hopping rule in an exploring period] When the ants are in the exploring period, they are all in the slow mode, $\sigma_j(t) \equiv s$. For $X_j(t) = (v_j(t), s)$, we define a set of nearest neighboring vertices of $v_j(t)$ as

$$\Lambda_j^s(t) := \begin{cases} \{v \in V_L : |v - v_j(t)| = 1\} = \{(1, 0), (0, 1)\}, & \text{if } v_j(t) = v_n, \\ \{v \in V_L : |v - v_j(t)| = 1, v \neq v_j(t - 1)\}, & \text{if } v_j(t) \in V_L \setminus \{v_n\}. \end{cases} \quad (2.11)$$

Then, at each time step $t \rightarrow t + 1$,

$$v_j(t) \rightarrow v \quad \text{with probability} \quad \frac{f(v, t)}{\sum_{w \in \Lambda_j^s(t)} f(w, t)}, \quad \text{if and only if } v \in \Lambda_j^s(t), \quad (2.12)$$

provided $\sum_{w \in \Lambda_j^s(t)} f(w, t) > 0$. If $\sum_{w \in \Lambda_j^s(t)} f(w, t) = 0$; that is, $f(v, t) = 0$ for all $v \in \Lambda_j^s(t)$, then

$$v_j(t) \rightarrow v \quad \text{with probability} \quad \frac{1}{|\Lambda_j^s(t)|}, \quad \text{if and only if } v \in \Lambda_j^s(t), \quad (2.13)$$

where $|\Lambda_j^s(t)|$ is the total number of vertices in $\Lambda_j^s(t)$. Note that the previous position $v_j(t - 1)$ is not included in $\Lambda_j^s(t)$ to prevent backward walking.

(Prohibition against cyclic motions) In an exploring period, if $v_j(t + 1) - v_j(t) \in \{(-1, 0), (0, -1)\}$, that is, the step is leftward or downward, hopping is regarded as a *retrograde motion*. We prohibit any succession of such retrograde motions to avoid the cyclic motions of walkers. When the particle is in the domain $\Gamma_{L,\ell}$, this prohibition rule is strengthened such that all downward steps are forbidden if $0 \leq x \leq \ell - 1$, and all leftward steps are forbidden if $L - \ell \leq y \leq L - 1$.

[Hopping rules in a homing period]

(Slow mode) For $X_j(t) = (v_j(t), s)$ in a homing period, we define a set of nearest neighboring vertices of $v_j(t)$ as

$$\tilde{\Lambda}_j^s(t) := \begin{cases} \{v \in V_L : |v - v_j(t)| = 1, v \neq v_j(t - 1)\}, & \\ \quad \text{if } v_j(t) \in V_L \setminus \{v_f\}, & \\ \{v \in V_L : |v - v_j(t)| = 1\} = \{(L - 2, L - 1), (L - 1, L - 2)\}, & \\ \quad \text{if } v_j(t) = v_f. & \end{cases} \quad (2.14)$$

Note that the previous position $v_j(t-1)$ is not included in $\tilde{\Lambda}_j^s(t)$ to prevent backward walking. Then, at each time step $t \rightarrow t+1$,

$$v_j(t) \rightarrow v \quad \text{with probability} \quad \frac{f(v,t)}{\sum_{w \in \tilde{\Lambda}_j^s(t)} f(w,t)}. \quad \text{if and only if } v \in \tilde{\Lambda}_j^s(t), \quad (2.15)$$

provided $\sum_{w \in \tilde{\Lambda}_j^s(t)} f(w,t) > 0$. If $\sum_{w \in \tilde{\Lambda}_j^s(t)} f(w,t) = 0$; that is, $f(v,t) = 0$ for all $v \in \tilde{\Lambda}_j^s(t)$, then

$$v_j(t) \rightarrow v \quad \text{with probability} \quad \frac{1}{|\tilde{\Lambda}_j^s(t)|}, \quad \text{if and only if } v \in \tilde{\Lambda}_j^s(t). \quad (2.16)$$

(Prohibition against cyclic motions) In a homing period, if $v_j(t+1) - v_j(t) \in \{(1,0), (0,1)\}$, that is, the step is rightward or upward, the hopping is regarded as a *retrograde motion*. We prohibit any succession of such retrograde motions to avoid the cyclic motions of walkers. When the particle is in the domain $\Gamma_{L,\ell}$, this prohibition rule is strengthened such that all rightward steps are forbidden if $L - \ell \leq y \leq L - 1$, and all upward steps are forbidden if $0 \leq x \leq \ell - 1$.

(Fast mode) For $X_j(t) = (v_j(t), f)$ in a homing period, we define a subset of the nearest neighboring vertices of $v_j(t)$ as

$$\tilde{\Lambda}_j^f(t) := \{v \in V_L : |v - v_j(t)| = 1, |v| < |v_j(t)|\}. \quad (2.17)$$

Then, in the time step $t \rightarrow t+1$,

$$v_j(t) \rightarrow v \quad \text{with probability} \quad \frac{1}{|\tilde{\Lambda}_j^f(t)|}, \quad \text{if and only if } v \in \tilde{\Lambda}_j^f(t). \quad (2.18)$$

Because we have considered the system in a subset V_L of the square lattice, $|\tilde{\Lambda}_j^f(t)| \in \{1, 2\}$. If $x = 0$ or $y = 0$ in $v_j(t) = (x, y)$, then, $|\tilde{\Lambda}_j^f(t)| = 1$, and hence, hopping in fast mode is deterministic.

(Switching) We introduce parameters $\gamma_{sf}, \gamma_{fs} \in [0, 1]$. Then, in time step $t \rightarrow t+1$ in the homing period, we change the mode of hopping as

$$\begin{aligned} \sigma_j(t) = s &\rightarrow f \quad \text{with probability } \gamma_{sf}, \\ \sigma_j(t) = f &\rightarrow s \quad \text{with probability } \gamma_{fs}. \end{aligned} \quad (2.19)$$

This implies that the mode does not change with probability $1 - \gamma_{sf}$ (resp. $1 - \gamma_{fs}$), when the particle is slow (resp. fast) modes at each time-point.

Remark Consider the extreme case with $\gamma_{sf} = 1$ and $\gamma_{fs} = 0$; hence, all particles are in fast mode in the homing period. In this case, the path length from v_f to v_n is fixed at the minimum value. Because our model is constructed on V_L given

by (2.1), the minimal path length is $2(L - 1)$. We notice that the total number of such optimal walks is 2^{L-1} and some of them are completely included in the Γ -region representing the ‘pheromone road’; an example is a Γ -shaped walk along the uppermost and leftmost edges of V_L . These paths are referred to as Γ -paths in Section 3.1. This is because of the simple square lattice discretization of the space which we adopted in our modeling. In the real experiments described in Section 1.2, as a matter of course, the Euclidean length of direct path between the food source and the nest is shorter than the length of ‘pheromone road’ as we can see in the lower picture for $\theta = 90^\circ$ in Fig. 1. Hence, purely visual-cues-mediated walks would not be realized in any trajectory trailing the ‘pheromone road’. In Section 3.1, we consider the opposite extreme case with $\gamma_{\text{sf}} = 0$ and $\gamma_{\text{fs}} = 1$. Because of our simple square lattice discretization of the space, some of the Γ -paths can have an optimal length $2(L - 1)$ as mentioned above; however, they were not observed in our simulations. All the observed Γ -paths are far from optimal. This phenomenon is caused by our setting so that the width of Γ -region, that is the number of ‘lanes’ in the Γ -region, is $\ell \geq 2$ and ‘lane changes’ are enhanced by the pheromone field, which make the Γ -paths include many redundant walk. In conclusion, simple square lattice discretization of the space allows us to simulate the transitions between the redundant Γ -paths and nearly optimal paths depending on the switching parameters γ_{sf} and γ_{fs} , which are expected from the experiments by the Nishimori group.

[Initial condition, update rule, random switching at food source, and time duration]

- (i) We consider an initial configuration such that all N particles are in the slow mode and start successively from the origin,

$$X_j(j - 1) = (0, s), \quad j = 1, \dots, N. \quad (2.20)$$

- (ii) We perform hopping of the particles and switch the mode in homing period sequentially according to the numbering of particles $j = 1, \dots, N$. The pheromone field is updated at each time step.
- (iii) When $v_j(t) = v_f$, that is, an ant arrives at the food source, switching between the slow and fast modes occurs randomly:

$$\sigma_j(t + 1) = \begin{cases} \text{s,} & \text{with probability } 1/2, \\ \text{f,} & \text{with probability } 1/2. \end{cases} \quad (2.21)$$

- (iv) Let $\tau(n)$ be the time duration such that the total number of particles which have returned to the nest v_n is n . We perform each numerical simulation up to the time step

$$T = \tau(\kappa N), \quad (2.22)$$

where κ denotes a parameter. That is, during T , totally κN particles shuttle between the nest and food source.

2.2 Parameter setting

We set the parameters concerning the time-dependent pheromone field as

$$f_0 = 1000, \quad f_1 = 0, \quad f_2 = 10, \quad q = 0.01. \quad (2.23)$$

We assume that the density of the particles is fixed as

$$\rho := \frac{N}{L^2} = \frac{1}{8} = 0.125, \quad (2.24)$$

the ratio of the width ℓ of the Γ -region defined by (2.6) with respect to L is given by

$$\frac{\ell}{L} = \frac{1}{20}, \quad (2.25)$$

and each simulation is performed for the time duration (2.22) with

$$\kappa = 4. \quad (2.26)$$

We have performed numerical simulations of the proposed stochastic model on square lattices of sizes $L = 40, 60,$ and 80 . In the present paper, we report the dependence of the simulation results on the switching parameters γ_{sf} and γ_{fs} which are changed in the interval $[0, 1]$. We have confirmed that the numerical results given below do not change qualitatively by changing the parameter settings (2.23)–(2.26). In particular, setting (2.26) for the time duration of each simulation is sufficient to observe stable distributions of the homing duration, which are reported in Section 3. The validity of the L -dependence of the parameters (2.24) and (2.25) is discussed in Section 4.1. A systematic study of the quantitative dependence of the model on parameters other than L, ℓ, N and γ_{sf} (with the relationship $\gamma_{fs} = 1 - \gamma_{sf}$) is considered as one of the future problems discussed in item (v) in Section 5. Table 1 summarizes the setting, changing, and fixed parameters of the present model.

3 Distributions of Homing Duration and Order Parameters

3.1 Γ -paths and order parameter \widetilde{M}

For each particle in the homing period, we trace the path from the food source v_f to nest v_n ,

$$\pi = \{v_f = v_0 \rightarrow v_1 \rightarrow v_2 \rightarrow \cdots \rightarrow v_A = v_n\}. \quad (3.1)$$

Here, the number of steps in π indicating the path length is expressed by A . In this study, we refer to the random variable A as the *homing duration*.

First, we consider the extreme case with $\gamma_{sf} = 0$ and $\gamma_{fs} = 1$. In this case all particles are in the slow mode following the ‘pheromone road’. Hence, all the paths in the homing period

Table 1: List of the setting, changing, and fixed parameters in the present discrete-time stochastic model on a square lattice

setting parameters		setting
L	system size	40, 60, 80
ℓ	width of the Γ -region	$L/20$
N	number of particles	$\rho L^2 = L^2/8$
changing parameters		range of value
γ_{sf}	switching probability from slow mode to fast mode	$[0, 1]$
γ_{fs}	switching probability from fast mode to slow mode	$[0, 1]$ or $1 - \gamma_{sf}$
fixed parameters		value
f_0	initial intensity of pheromone in the Γ -region	1000
f_1	amount of pheromone dropped by an exploring particle	0
f_2	amount of pheromone dropped by a homing particle	10
q	evaporation rate of pheromone	0.01
κ	time duration of simulation $T = \tau(\kappa N)$	4

are completely included in the Γ -region, $\Gamma_{L,\ell}$, as defined by (2.6). Generally, if the path in the homing period is completely included in the Γ -region, we say that the path is a Γ -path. (See Fig.2.) In this extreme case, we write the random variable of the homing duration as A_0 by putting the subscript 0. Figure 3 shows a typical distribution of the homing duration A_0 in one simulation sample for a system of size $L = 60$. We note that the minimum value of the homing duration is $2(L-1) = 118$, which is realized, for example, by a Γ -shaped homing walk along the uppermost edges and then the leftmost edges of V_L . However, the observed distribution of A_0 in this simulation centered at a larger value $\simeq 189$. This implies that slow mode paths are far from optimal and include many redundant walks which are enhanced by the pheromone field. In the observed distribution, we measured width ΔA_0 defined as the difference between the observed maximum and minimum values of A_0 . We calculated the average value $\langle \Delta A_0 \rangle$ for several numerical-simulation samples. The results are as follows:

$$\begin{aligned}
 \langle \Delta A_0 \rangle &= 26.6 \pm 1.8, & \text{for } L = 40, \\
 \langle \Delta A_0 \rangle &= 41.6 \pm 2.7, & \text{for } L = 60, \\
 \langle \Delta A_0 \rangle &= 54.4 \pm 3.2, & \text{for } L = 80,
 \end{aligned} \tag{3.2}$$

where the errors are given by the standard deviations over ten samples of numerical simulations for systems of sizes $L = 40$ and 60, and five samples for the system of size $L = 80$. The above results show a linear dependence of $\langle \Delta A_0 \rangle$ on L ,

$$\langle \Delta A_0 \rangle \simeq 0.7L - 0.83, \tag{3.3}$$

as shown by Fig.4.

We define \widetilde{M} as the ratio of the number of observed particles following Γ -paths to the total number of homing particles in the simulation; *i.e.* $\kappa N = \kappa L^2/8$;

$$\widetilde{M} := \frac{\#\{\text{homing particle following a } \Gamma\text{-path}\}}{\kappa N}. \tag{3.4}$$

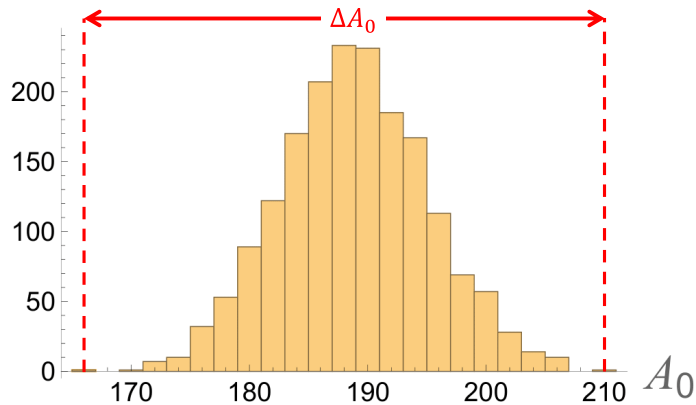


Figure 3: Histogram of the homing duration A_0 of particles in one simulation sample, when $(\gamma_{sf}, \gamma_{fs}) = (0, 1)$, in a system of size $L = 60$. All particles are in slow mode and trail Γ -paths. In this observed distribution, the mean of A_0 is 188.9, the maximum and minimum values are 210 and 166, respectively, and hence, $\Delta A_0 = 44$.

As previously mentioned, $\widetilde{M} = 1$, if $(\gamma_{sf}, \gamma_{fs}) = (0, 1)$.

From now on, we assume the relationship

$$\gamma_{sf} + \gamma_{fs} = 1. \quad (3.5)$$

As γ_{sf} increases from 0, \widetilde{M} decreases from 1, since particles in the fast mode appear and they make deviation from the ‘pheromone road’. In other words, \widetilde{M} plays the role of the *order parameter* for the path selection which persists the original ‘pheromone road’ in the homing period.

3.2 Nearly optimal paths and order parameter M

For a system of size $L = 60$, Fig. 5 (a) shows the dependence of the distribution of the homing duration A on γ_{sf} with relation (3.5). When $\gamma_{sf} \gtrsim 0.3$, Γ -path is no longer observed and the observed paths are dominated by *non- Γ -paths*. As γ_{sf} increases, the observed support of the distribution of the homing duration for the non- Γ -paths shifts to lower value region of A . This means that as γ_{sf} increases, more pioneer walkers appear to build shorter paths from the food source to nest because particles can be in the fast mode more frequently. In addition to the left shift, Fig. 5 (a) shows that the bell-shaped distribution of A for the non- Γ -paths becomes sharper as γ_{sf} increases. The monotonic decrease in the mean $\langle A \rangle$ and standard deviation σ of the distribution of A with the increment of γ_{sf} is shown in Fig. 5 (b) for the non- Γ -paths. This implies that shorter paths are strengthened by the followers of pioneer walkers via interactions through the pheromone field. As γ_{sf} approaches one, the distribution quickly sharpens and appears to condense to the shortest value of A , *i.e.* the length of the optimal path, $2(L - 1) = 118$. In other words, as γ_{sf} approaches 1, a large

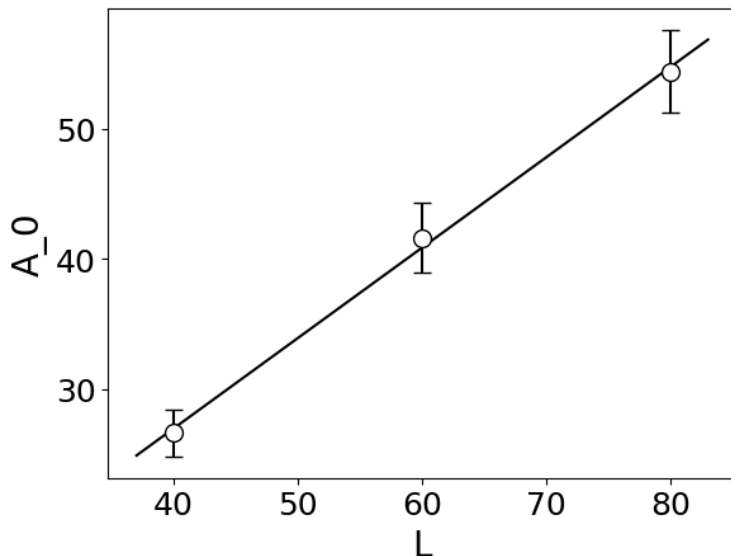


Figure 4: The dependence of $\langle \Delta A_0 \rangle$ on L is well described by a linear fitting; $\langle \Delta A_0 \rangle \simeq 0.7L - 0.83$. The errors are given by standard deviations over ten samples of numerical simulation for systems of sizes $L = 40$ and 60 , and five samples for the system of size $L = 80$.

number of particles tend to trail through paths which are very close to the optimal path. We want to call such paths nearly optimal paths.

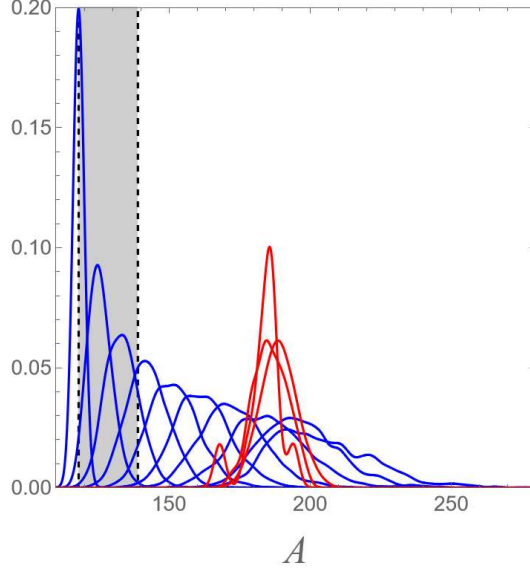
To define nearly optimal paths, we use the value $\langle \Delta A_0 \rangle$ determined by the homing duration distribution when $(\gamma_{sf}, \gamma_{fs}) = (0, 1)$ in Section 3.1. If the homing duration A of the path satisfies the condition

$$2(L - 1) \leq A \leq 2(L - 1) + \frac{1}{2}\langle \Delta A_0 \rangle, \quad (3.6)$$

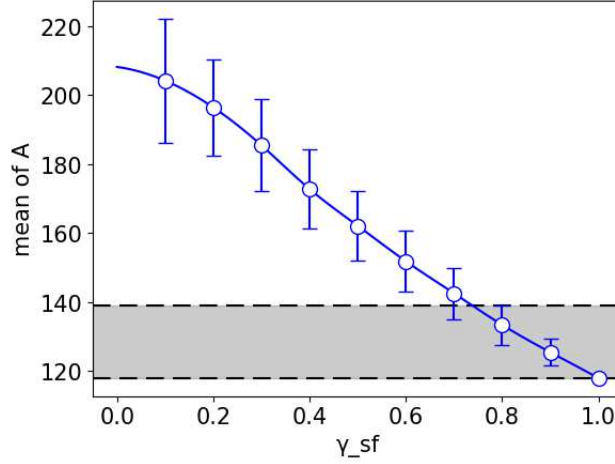
then we say that it is a *nearly optimal path*. The range (3.6) of A is indicated by the shaded regions in Figs. 5 (a) and (b). Then, we define another order parameter M in addition to \widetilde{M} as the ratio of the number of particles following nearly optimal paths in a homing period to the total number of homing particles in the simulation, κN ,

$$M := \frac{\#\{\text{homing particle following a nearly optimal path}\}}{\kappa N}. \quad (3.7)$$

Figure 2 illustrates an example of Γ -path which contributes to the order parameter \widetilde{M} and two examples of nearly optimal paths which contribute to the order parameter M . We will compare the dependence on γ_{sf} of these two types of order parameters M and \widetilde{M} varying the system size L . The choice of $\langle \Delta A_0 \rangle / 2$ as the width in the condition (3.6) which defines the nearly optimal path is to make the dependence of M on L comparable with that of \widetilde{M} . The definitions (3.6) and (3.7) work well, as shown below.



(a) Dependence on γ_{sf} with the relationship $\gamma_{fs} = 1 - \gamma_{sf}$ of the distributions of homing duration A of Γ -paths (shown by red curves) and of non- Γ -paths (by blue curves) for the system with $L = 60$. Three distributions of A are shown for the Γ -paths with $\gamma_{sf} = 0, 0.1, \text{ and } 0.2$, and ten for the non- Γ -paths with $\gamma_{sf} = 0.1, 0.2, 0.3, 0.4, 0.5, 0.6, 0.7, 0.8, 0.9, \text{ and } 1$. In both the cases, the right edge (the point at which the right tail of the distribution becomes zero) decreases monotonically as γ_{sf} increases.



(b) The means of the distribution of A for non- Γ -paths (shown by the blue circles in (a)) are plotted against $\gamma_{sf} \in (0, 1]$. The standard deviations of the distribution of A are indicated by error bars.

Figure 5: Distributions of the homing duration A . The shaded region indicates the range of A , $2(L - 1) \leq A \leq 2(L - 1) + \langle \Delta A_0 \rangle / 2$, for the nearly optimal paths. For $L = 60$, $2(L - 1) = 118$ and $\langle \Delta A_0 \rangle / 2 = 20.8$ by (3.2).

4 Phase Transitions and Critical Phenomena in Path Selections

4.1 Almost data-collapse with respect to system size

Using the relation between the parameters (3.5), Fig.6 (a) shows that the γ_{sf} -dependence of the two types of order parameters, M and \widetilde{M} , for systems of different sizes, $L = 40, 60$, and 80 . For systems of sizes, $L = 40$ and 60 , (resp. 80) we have obtained 10 samples (resp. 3 samples) for each parameter $\gamma_{\text{sf}} \in [0, 1]$. These lines interpolate the average values of the samples. We have confirmed that the standard deviations are very small, *e.g.* 3.0×10^{-3} for M at $\gamma_{\text{sf}} = 0.6$ and 1.5×10^{-2} for \widetilde{M} at $\gamma_{\text{sf}} = 0.1$ for $L = 60$. Hence, the error bars are omitted, as shown in Fig.6 (a). By definition, $\widetilde{M} \rightarrow 1$ as $\gamma_{\text{sf}} \rightarrow 0$, and $M \rightarrow 1$ as $\gamma_{\text{sf}} \rightarrow 1$. We observe that when γ_{sf} is small, $M = 0$ and $\widetilde{M} > 0$, and when γ_{sf} is large, $M > 0$ and $\widetilde{M} = 0$. The rapid decrease in \widetilde{M} around $\gamma_{\text{sf}} \simeq 0.1$, and the rapid increase in M around $\gamma_{\text{sf}} \simeq 0.6$ indicate the global switching phenomena of path selection between the Γ -paths and nearly optimal paths.

Figure 6 (a) shows that the differences in the values of M and \widetilde{M} caused by increasing the system size L are relatively small. Roughly speaking, this fact is regarded as a kind of *data collapse* that shows the independence of global switching phenomena in path selections on size L in the proposed model. That is, the settings for the number of particles, $N = \rho L^2 \propto L^2$, as given by (2.24), the width of the Γ -region ('pheromone road'), $\ell = L/20 \propto L$, given by (2.25), and the condition (3.6) for nearly optimal paths using the quantity, $\langle \Delta A_0 \rangle \simeq aL + b$, (see (3.3)) are simple, but they provide a *proper scaling property* of the system with respect to the change in the system size L .

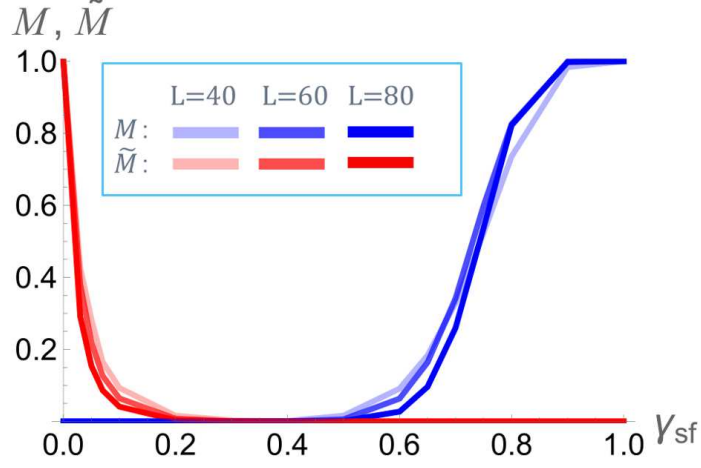
4.2 Evaluations of critical values and critical exponents

In contrast, in the vicinity of the values of γ_{sf} at which \widetilde{M} approaches zero ($\gamma_{\text{sf}} \simeq 0.1$) and M emerges ($\gamma_{\text{sf}} \simeq 0.6$), the changes show systematic dependence on L . This observation suggests that we will have *critical phenomena* in the $L \rightarrow \infty$ limit and that the present global switching phenomena in path selection can be considered as *continuous phase transitions*.

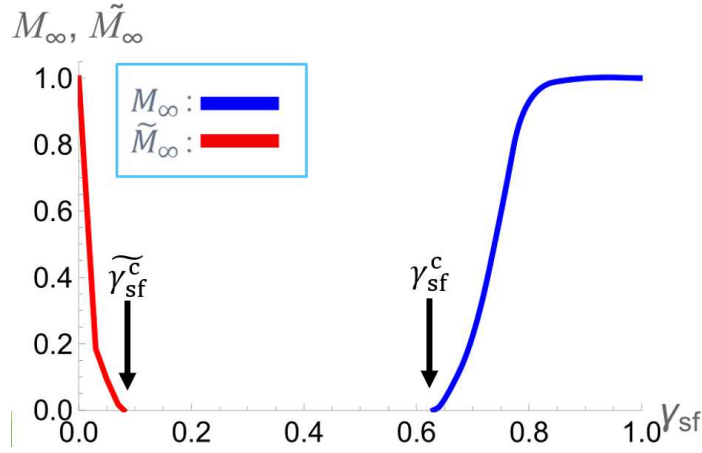
To explain our method for estimating the order parameters in the $L \rightarrow \infty$ limit, we write the order parameters as M_L and \widetilde{M}_L for a system of size L . At each value of $\gamma_{\text{sf}} \in [0, 1]$ with (3.5) we assume the following simple dependence of the order parameters on system size L ,

$$M_\infty = M_L + \frac{c_1}{L}, \quad \widetilde{M}_\infty = \widetilde{M}_L + \frac{\widetilde{c}_1}{L}, \quad \text{as } L \rightarrow \infty, \quad (4.1)$$

where c_1 and \widetilde{c}_1 are fitting parameters, and M_∞ and \widetilde{M}_∞ are the estimated values of the order parameters of an infinite system. (See item (ii) in Section 5 for a possible improvement by introducing the critical exponents ν and $\widetilde{\nu}$.) By plotting the values of M_L (resp. \widetilde{M}_L) with respect to $1/L$, the $L \rightarrow \infty$ limit of the order parameter M_∞ (resp. \widetilde{M}_∞) is evaluated using the 'y-intercept'. The estimated curves of M_∞ and \widetilde{M}_∞ are shown for $\gamma_{\text{sf}} \in [0, 1]$ in Fig. 6 (b).

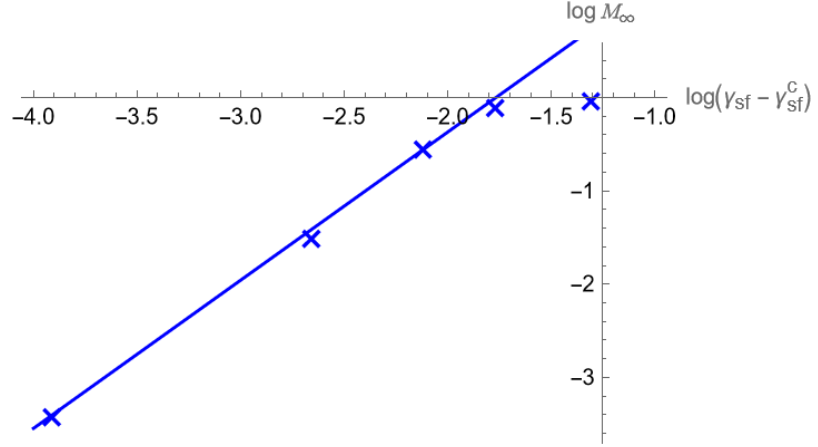


(a) For each value of γ_{sf} , we put $\gamma_{fs} = 1 - \gamma_{sf}$ and numerically evaluated the order parameters M_L and \tilde{M}_L for the three systems of sizes $L = 40, 60,$ and 80 , as explained in Section 4.1. A total of $2 \times 3 = 6$ curves are plotted versus γ_{sf} in different colors.

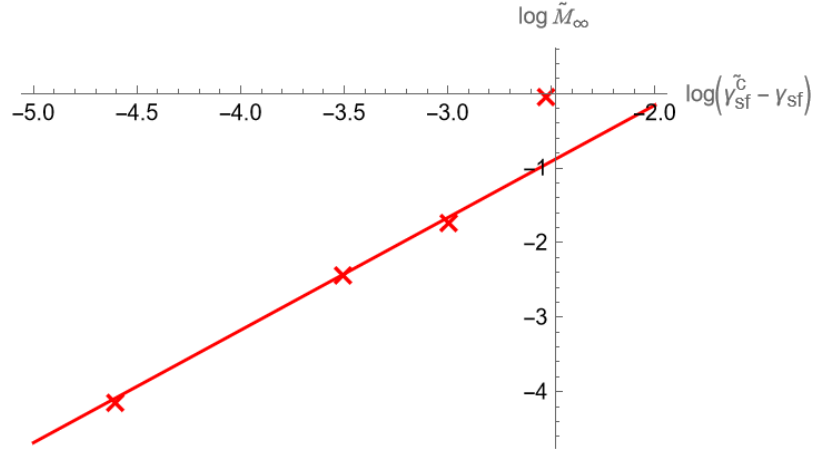


(b) M_∞ and \tilde{M}_∞ for an infinite system are estimated using $1/L$ -plots, as described in Section 4.2. The critical values $\gamma_{sf}^c \simeq 0.63$ and $\tilde{\gamma}_{sf}^c \simeq 0.08$ are indicated by the arrows.

Figure 6: The order parameters M and \tilde{M} are plotted against $\gamma_{sf} \in [0, 1]$, where $\gamma_{fs} = 1 - \gamma_{sf}$.



(a) Fitting with $\gamma_{\text{sf}}^c = 0.63$ and $\beta = 1.59$ for M_∞ .



(b) Fitting with $\tilde{\gamma}_{\text{sf}}^c = 0.08$ and $\tilde{\beta} = 1.51$ for \tilde{M}_∞ .

Figure 7: Log-log plots of the order parameters M_∞ and \tilde{M}_∞ with respect to the deviations of the parameter γ_{sf} from its critical values, $\gamma_{\text{sf}} - \gamma_{\text{sf}}^c$ and $\tilde{\gamma}_{\text{sf}}^c - \gamma_{\text{sf}}$, respectively. The slopes provide the critical exponents β and $\tilde{\beta}$.

The results suggest that we can define the two types of critical values of γ_{sf} according to the two types of order parameters, M_∞ and \widetilde{M}_∞ , as

$$\gamma_{\text{sf}}^c := \inf\{\gamma_{\text{sf}} : M_\infty > 0\}, \quad \widetilde{\gamma}_{\text{sf}}^c := \sup\{\gamma_{\text{sf}} : \widetilde{M}_\infty > 0\}. \quad (4.2)$$

From the $1/L$ -plots, we evaluate the critical values as follows:

$$\gamma_{\text{sf}}^c \simeq 0.63, \quad \widetilde{\gamma}_{\text{sf}}^c \simeq 0.08. \quad (4.3)$$

See Fig. 6 (b).

The continuous changes in M and \widetilde{M} at these critical points suggest that the phase transitions are continuous. The critical phenomena are then described by the following *power laws* as functions of the parameter γ_{sf} ,

$$\begin{aligned} M_\infty(\gamma_{\text{sf}}) &\simeq c_2(\gamma_{\text{sf}} - \gamma_{\text{sf}}^c)^\beta, & \gamma_{\text{sf}} &\gtrsim \gamma_{\text{sf}}^c, \\ \widetilde{M}_\infty(\gamma_{\text{sf}}) &\simeq \widetilde{c}_2(\widetilde{\gamma}_{\text{sf}}^c - \gamma_{\text{sf}})^{\widetilde{\beta}}, & \gamma_{\text{sf}} &\lesssim \widetilde{\gamma}_{\text{sf}}^c, \end{aligned} \quad (4.4)$$

where β and $\widetilde{\beta}$ are the *critical exponents of order parameters* M and \widetilde{M} , respectively [1, 9, 12]. As shown in Fig.7, the power laws are observed and the log-log plots provide the values

$$\beta \simeq 1.6, \quad \widetilde{\beta} \simeq 1.5. \quad (4.5)$$

5 Concluding Remarks and Future Problems

At the end of this paper, we list out the concluding remarks and possible future problems.

- (i) The interactions between the ants are given by the pheromone field, which evolves over time and is affected by the previous behaviors of other ants. In this study, we have investigated such an interacting particle system by numerically simulating a cellular automaton model. What theory is relevant for describing such temporally inhomogeneous interactions with memory effects?
- (ii) In the *finite-size scaling theory* [1, 9, 12], $1/L$ -fitting (4.1) should be refined by introducing the exponents ν and $\widetilde{\nu}$ as follows:

$$M_\infty = M_L + \frac{c'_1}{L^\nu}, \quad \widetilde{M}_\infty = \widetilde{M}_L + \frac{\widetilde{c}'_1}{L^{\widetilde{\nu}}}, \quad \text{as } L \rightarrow \infty, \quad (5.1)$$

at each value of $\gamma_{\text{sf}} \in [0, 1]$ with (3.5), where c'_1 and \widetilde{c}'_1 are the fitting parameters, and M_∞ and \widetilde{M}_∞ are the estimated values of the order parameters for an infinite system. In this study, we have obtained the numerical results for only three sizes: $L = 40$, 60, and 80. Hence, it is difficult to evaluate the values of ν and $\widetilde{\nu}$ using numerical fitting. We have assumed the mean-field value $\nu = \widetilde{\nu} = 1$ in the fitting (4.1). The numerical results (4.5) suggest $\beta = \widetilde{\beta} = 3/2$. A systematic study on finite-size scaling based on large-scale simulations will be an important future problem. The correlation

and response functions of the present model for the group behavior of ants should be carefully considered. They need to understand the critical phenomena described by the critical exponents ν and γ for the divergence of the correlation length and response functions, respectively, and δ for the power-law at the critical points.

- (iii) An effective theory is required to describe the phase transitions and critical phenomena in path selection for foraging ants. As mentioned in item (ii) above, we first try to establish the mean-field theory. Fractional values of critical exponents suggest the emergence of *fractal structures* in paths of ants at the moment when the nearly optimal paths are first established, as well as at the moment when the ‘pheromone road’ vanishes during the path selection of the ants.
- (iv) By the definition (2.19), parameters γ_{sf} and γ_{fs} can take any values in $[0, 1]$ independently. We have assumed in the present paper, however, the special relation (3.5) between these two parameters. The present study on the global switching of path selections shall be generalized to the whole parameter space $(\gamma_{sf}, \gamma_{fs}) \in [0, 1]^2$. As a result, we will obtain the *phase diagram* showing three types of phases; (a) the phase in which homing particles select the Γ -paths (*i.e.* trailing paths of the ‘pheromone road’) indicated by $\widetilde{M} > 0$ and $M = 0$, (b) the phase in which homing particles select the nearly optimal paths indicated by $\widetilde{M} = 0$ and $M > 0$, and (c) the intermediate phase.
- (v) As shown in Table 1, we have fixed many parameters except L, ℓ, N and γ_{sf} with relation (3.5). A more general and systematic study of the proposed model is required to investigate the dependence of the results on other parameters. For example, if we change the parameter κ , the time duration of the numerical observation is changed. Then, the transient or relaxation phenomena in the initial time period and the long-term behavior of the present processes are clarified. It is an interesting research subject to study the precise dependence of the results on the evaporation rate q of the pheromone, because this parameter controls the spatiotemporal correlations between particles via the pheromone field.
- (vi) The present study was motivated by the experiments reported by the group of the last author (HN) of this paper, as briefly explained in Section 1.2 [10]. In our modeling, we adopted the setting with $\theta = 90^\circ$ for the turning angle of the ‘pheromone road’. (See Figs. 1 and 2 again.) This is because no global switching phenomena in the path selection were observed in the other settings with $\theta = 45^\circ$ and $\theta = 60^\circ$. In the present model, we have introduced other parameters γ_{sf} and γ_{fs} (the switching parameters between the fast and slow modes) and showed that the global switching phenomena in path selection are realized as continuous phase transitions associated with critical phenomena at critical values γ_{sf}^c and $\widetilde{\gamma}_{sf}^c$. This result suggests that even if we adopt a setting of $\theta = 45^\circ$ or $\theta = 60^\circ$, we will be able to observe such phase transitions provided that we properly choose the parameters γ_{sf} and γ_{fs} . To simulate the models by setting $\theta = 45^\circ$ or $\theta = 60^\circ$ efficiently, we shall change the lattice from the square lattice to the triangular or the honeycomb lattices. We expect that the critical phenomena

associated with the phase transitions representing the global switching phenomena in path selections are *universal* and do not depend on any details of the lattice structure. If so, the present study on lattice models will provide the universal statements to the path selection phenomena observed in real foraging ants.

Acknowledgements The authors would like to express their gratitude to Mitsugu Matsushita, Frank den Hollander, Helmut R. Brand, Piotr Graczyk, Gregory Schehr, and Hirohiko Shimada for their valuable discussions on this work. This study was carried out under the Open-Type Professional Development Program of the Institute of Statistical Mathematics, Tokyo (2023-ISMHRD-7010). Part of this study was presented by AE on December 6, 2023, at the Institute for Mathematical Sciences, National University of Singapore. AE, SM, YT, and MK are grateful to Akira Sakai and Rongfeng Sun for organizing the three-week fruitful program in December 2023. Additionally, this work received support from the Research Institute for Mathematical Sciences, an International Joint Usage/Research Center located at Kyoto University. MK is funded by the Grant-in-Aid for Scientific Research (C) (No.24K06888), (C) (No.19K03674), (B) (No.23K25774), (B) (No.23H01077), (A) (No.21H04432), and the Grant-in-Aid for Transformative Research Areas (A) (No.22H05105) of the Japan Society for the Promotion of Science (JSPS). HN is supported by the Grant-in-Aid for Scientific Research (B) (No.20H01871), and the Grant-in-Aid for Transformative Research Areas (A) (No.21H05293) and (A) (No.21H05297) of JSPS.

References

- [1] B. Chopard, M. Droz, Cellular Automata Modeling of Physical Systems, Cambridge University Press, Cambridge, UK, 1998.
- [2] F. den Hollander, S. Nandan, Spatially inhomogeneous populations with seed-banks: I. Duality, existence and clustering, *J. Theor. Probab.* **35** (2022) 1792–1841.
- [3] F. den Hollander, S. Nandan, Spatially inhomogeneous populations with seed-banks: II. Clustering regime, *Stochastic Process. Appl.* **150** (2022) 116–146.
- [4] S. Floreani, C. Giardinà, F. den Hollander, S. Nandan, F. Redig, Switching interacting particle systems: Scaling limits, uphill diffusion and boundary layer, *J. Stat. Phys.* **186** (2022) 33 (45 pages).
- [5] A. Greven, F. den Hollander, M. Oomen, Spatial populations with seed-bank: Well-posedness, duality and equilibrium, *Electron. J. Probab.* **27** (18) (2022) 1–88.
- [6] A. Greven, F. den Hollander, M. Oomen, Spatial populations with seed-bank: Renormalisation on the hierarchical group, to appear in *Memoirs of AMS*. [arXiv:math.PR/2110.02714](https://arxiv.org/abs/math.PR/2110.02714)

- [7] B. Hölldobler, E. O. Wilson, *The Ants*, Harvard University Press, Cambridge, MA, 1990.
- [8] J. T. Lennon, F. den Hollander, M. Wilke-Berenguer, J. Blath, Principle of seed banks and the emergence of complexity from dormancy, *Nat. Commun.* **12** (2021) 4807 (16 pages).
- [9] J. Marro, R. Dickman, *Nonequilibrium Phase Transitions in Lattice Models*, Cambridge University Press, Cambridge, UK, 1999.
- [10] Y. Ogihara, O. Yamanaka, T. Akino, S. Izumi, A. Awazu, H. Nishimori, Switching of primarily relied information by ants: A combinatorial study of experiment and modeling, in: (eds.) T. Ohira, T. Uzawa (Eds.), *Mathematical Approaches to Biological Systems – Networks, Oscillations, and Collective Motions*, Springer-Verlag, 2015, pp.119–137.
- [11] S. Shinoda, *Analysis of the influence of visual cues for foraging ants (in Japanese)*. Graduate Thesis, Department of Mathematics, Hiroshima University, 2013.
- [12] T. Vicsek, A. Zafeiris, Collective motion. *Phys. Rep.* **517** (2012) 71–140.